CHEMISTRY
A EUROPEAN JOURNAL

DOI: 10.1002/chem.200800416

The Role of Crystallization Parameters for the Synthesis of Germanosilicate with UTL Topology

Oleksiy V. Shvets,[a, b] Arnošt Zukal,[a] Natalia Kasian,[b] Naděžda Žilková,[a] and Jiří Čejka*[a]

Abstract: The investigation of the critical synthesis parameters of germanosilicate of UTL topology, possessing 14- and 12-rings, has been carried out in detail. (6*R*,10*S*)-6,10-Dimethyl-5-azoniaspiro[4.5]decane hydroxide was used as the structure-directing agent (SDA). The kinetics of the synthesis, the role of the Si/Ge ratio in the synthesis mixture, and the effect of the calcination procedure were investigated in relation to the crystallinity and textural properties of the synthesized material. The optimum synthesis time was found to be six days for Si/Ge and (Si+Ge)/SDA molar ratios of 2 and 1.7, respectively. The UTL zeolite crystallizes as small sheets of 10 μm in size. The micropore volume of the best crystals is 0.22 $cm^3 g^{-1}$ with a micropore diameter of 1.05 nm, based on DFT and Saito–Foley analyses of adsorption data.

Keywords: azo compounds · germanium · microporous materials · structure elucidation · zeolites

Introduction

Crystalline molecular sieves, with an extra-large pore diameter of their channels and high sorption capacity, possess a particular potential for applications in adsorption and catalysis. Among such materials, a special position is held by zeolites as the most frequently employed heterogeneous catalysts in the chemical industry.[1] The most important features for catalytic applications of zeolites involve well-defined structures with micropore channels, a chemical composition able to introduce catalytic active centers, and environmental tolerance.[2] Although zeolite-based catalysts are used in almost half of all large-scale technological units,[3] their main limitations are due to the restricted size of their channels, which are not larger than 1 nm.[4] Zeolites are frequently applied as catalysts in the transformations of aromatic hydrocarbons through alkylation, disproportionation, and isomerization[5–9] or acylation[10,11] reactions; for this reason, any increase in the size of channels would be desirable.

Recently, particular attention has been focused on the development of new synthetic strategies for the preparation of extra-large pore zeolites and zeotypes based on silicates, phosphates, and germanates.[12] Though germanate zeotypes have been synthesized in a large variety of structures with high porosity, the potential for their industrial application is not promising because of their high cost and low thermal and hydrolytic stability. Until now, the only synthesized extra-large-pore zeolites are 14-ring materials like CIT-5,[13] UTD-1,[14] SSZ-53 and SSZ-59,[15] and gallosilicate 18-ring ECR-34,[16] all containing one-dimensional channel systems, and germanosilicate 18-ring ITQ-33[17] with a two-dimensional system of perpendicular 18- and 10-ring channels. The synthesis of extra-large-pore zeolites could be an important alternative to the synthesis of mesoporous zeolites[18] or micro/mesoporous composite materials.[19]

Recently, two independent research groups have synthesized the germanosilicate zeolites ITQ-15 and IM-12, which possess a two-dimensional system of perpendicular 12-ring and 14-ring channels of diameter 8.5×5.5 and 9.5×7.1 Å, respectively.[20,21] The zeolite ITQ-15 was prepared using 1,1,3-trimethyl-6-azonia-tricyclo-[3.2.1.$4^{6,6}$]decane hydroxide as the structure-directing agent (SDA). The zeolite IM-12 was synthesized using (6*R*,10*S*)-6,10-dimethyl-5-azoniaspiro-[4.5]decane hydroxide. The Si/Ge ratio in these zeolites was relatively low: 8.5 and 4.5 for ITQ-15 and IM-12, respective-

[a] Dr. O. V. Shvets, Dr. A. Zukal, Dr. N. Žilková, Prof. J. Čejka
J. Heyrovský Institute of Physical Chemistry
Academy of Sciences of the Czech Republic v.v.i.
Dolejškova 3, 182 23 Prague 8 (Czech Republic)
Fax: (+420) 286-582-307
E-mail: jiri.cejka@jh-inst.cas.cz

[b] Dr. O. V. Shvets, Dr. N. Kasian
L. V. Pisarzhevsky Institute of Physical Chemistry
National Academy of Sciences of Ukraine
Pr. Nauky 31, 03037 Kyiv (Ukraine)

ly. The code UTL was assigned to this zeolite topology by the International Zeolite Association. Based on the detailed structural investigation, it seems that the key structural building units are double 4-rings (D4R), the formation of which is favored by the presence of germanium atoms in the reaction mixture.[22,23] Similar secondary building units are typical for other germanosilicate zeolites, including ITQ-22,[24] ITQ-17,[22] ITQ-27,[25] and ITQ-33.[17] Atomistic force field methodology confirmed the predicted almost exclusive location of Ge in D4Rs, which are the characteristic secondary structural units in all new ITQ zeolites synthesized with Ge.[26] As the Si/Ge ratio is not too low, these zeolites are characterized by a relatively high thermal and hydrolytic stability. After the introduction of heteroatoms bearing catalytic activity, for example Ti or Sn,[27] efficient catalysts can be obtained. For example, with the introduction of aluminum inducing the formation of acid sites in UTL zeolite in higher concentrations, an (Si+Ge)/Al ratio lower than 20 would allow the tailoring of the zeolite hydrophobicity/hydrophilicity as well as the ion-exchange properties, particularly towards divalent cations. Also, the decrease in the concentration of Ge in the structure without a loss of crystallinity, and the incorporation of other cations, such as Ga^{3+} or Fe^{3+}, are problems which remain to be solved.

Considering the specified features of the crystal structure and porous system of germanosilicate zeolite with UTL topology, we carried out a detailed investigation of the crucial synthesis parameters with the following objectives: 1) determination of the ranges of Si/Ge and (Si+Ge)/SDA ratios required for the synthesis of UTL structures using (6*R*,10*S*)-6,10-dimethyl-5-azoniaspiro[4.5]decane hydroxide as the structure-directing agent, 2) estimation of the kinetics of the synthesis, 3) detailed description of the calcination procedure of UTL zeolite, and 4) investigation of porous structure parameters.

Results and Discussion

Characterization of all synthesized and calcined zeolites was performed by using X-ray powder diffraction. Figure 1 (left) provides a comparison of the X-ray powder diffraction patterns of as-synthesized UTL zeolites prepared with different Si/Ge and (Si+Ge)/SDA molar ratios in the reaction mixture at the synthesis temperature of 175 °C. It is clearly seen that zeolites with UTL topology were prepared with a high crystallinity and without the presence of any other amorphous or crystalline phases in the initial range of Si/Ge higher than 2 and lower than 5, with the ratio (Si+Ge)/SDA varying from 1.7 to 4. When a Si/Ge = 1 ratio was used in the reaction mixture, the synthesis resulted in the formation of a mixture of UTL zeolite and β-GeO_2. The increase in the Si/Ge ratio from

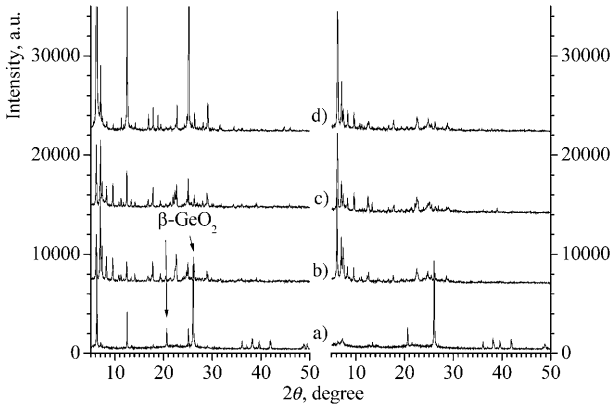

Figure 1. X-ray diffraction patterns of as-synthesized (left) and calcined (right) germanosilicate UTL prepared with template (6R,10S)-6,10-dimethyl-5-azoniaspiro[4.5]decane hydroxide with different Si/Ge and (Si+Ge)/SDA ratios: a) 1 and 4; b) 2 and 4; c) 2 and 1.7; d) 5 and 4, respectively.

2 to 5 substantially changes the relationship between the intensities of the individual diffraction lines. The higher the Si/Ge ratio, the more intense are the diffraction lines at 6.23, 12.50, 18.80, and 25.6°, which correspond to the d_{200}, d_{400}, d_{600}, and d_{800} planes, respectively. This is in agreement with X-ray patterns published by Corma et al.[20] and Paillaud et al.[21] Ge is expected to be preferentially located in D4Rs in analogy to other zeolites[28–30] and all indicated diffraction lines cross the centers of D4R units. However, the increase in the intensity of these diffraction lines could be explained in terms of the preferential orientation of the crystal plates of UTL zeolite, despite our efforts to avoid such a preference by careful packing of the sample into the holder.

The real chemical composition of the zeolite samples is shown in Table 1. If the Si/Ge ratio is 4.17 and 9.44 then the proportion of germanium atoms in the UTL framework is equal to 14.7 and 7.3 atoms per unit cell or per 16 positions in two D4R units. The sharp increase in the intensity of the specified diffraction lines is probably a result of a population change in the centers of polyhedrons in a D4R and a displacement of oxygen atoms.

Calcination of UTL zeolites led to significant changes in the intensity of X-ray diffraction lines (Figure 1, right). XRD patterns of UTL zeolites synthesized with the highest concentration of Ge (Si/Ge = 1) were clear evidence for the partial structural collapse of these samples during calcina-

Table 1. Chemical compositions of reaction mixtures (RMs) and corresponding UTL samples.

	Initial molar ratio				Si/Ge	Si/Ge	(Si+Ge)/SDA	Contents in samples, wt%	
	Si	Ge	SDA	H_2O	in RM	in samples	in RM	SDA	H_2O
UTL/1	0.80	0.40	0.3	30	2	4.17	4	12.56	3.67
UTL/2	0.80	0.40	0.7	30	2	4.18	1.7	12.73	3.36
UTL/3	0.80	0.40	0.4	30	2	4.17	3	12.96	3.32
UTL/4	0.80	0.40	0.6	30	2	4.19	2	12.48	3.66
UTL/5	1.00	0.20	0.3	30	5	9.44	4	12.60	2.81
UTL/6	0.60	0.60	0.3	30	1	4.17	4	4.52	8.10

tion. The dominant diffraction lines remaining after calcination of this zeolite can be attributed to β-GeO_2 or isostructural α-quartz. Some differences between the XRD results of UTL zeolites with Si/Ge from 2 to 5 were observed. Mainly, they manifested a decreasing intensity of the diffraction lines, and as a result the XRD patterns of the calcined samples with Si/Ge > 4 become similar.

For a better understanding of the reaction conditions leading to the pure well-crystalline UTL zeolite we followed the kinetics of the synthesis. Figure 2 shows XRD patterns

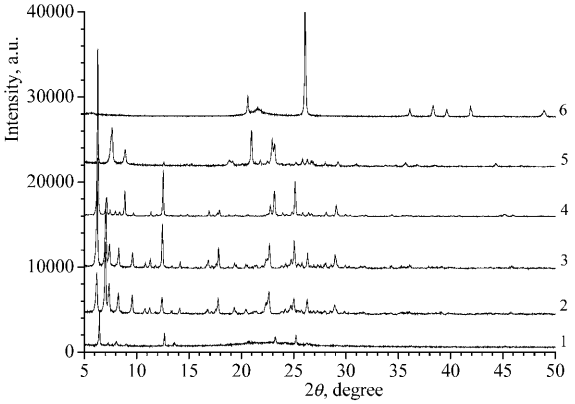

Figure 2. X-ray diffraction patterns of germanosilicate UTL with Si/Ge = 2 and (Si + Ge)/SDA = 4 after different times of the synthesis: 1) 3, 2) 4, 3) 6, 4) 8, 5) 10, and 6) 14 days.

of UTL zeolite synthesized with an initial Si/Ge ratio equal to 2 and (Si + Ge)/SDA = 4 for different times of the synthesis. It is clearly seen that after just one day of the synthesis at 175 °C some diffraction lines of UTL structure appeared. The intensity of these diffraction lines increases with the prolongation of the synthesis time, and it seems that the maximum intensity (optimum synthesis time under reaction conditions used) is after about six days (Figure 2, curve 3). Further prolongation of the synthesis time led to the appearance of diffraction lines of another more dense zeolite possessing MTW topology, with characteristic diffraction lines at 7.65, 8.87, 20.97°, and so forth. This confirms the progress of the transformation of the less dense UTL structure into the more condensed one of MTW. After ten days of the synthesis the MTW zeolite is the prevailing material in the reaction mixture, and after 14 days quartz is preferentially formed.

Figure 3 provides a scheme of the time evolution of the content of UTL, MTW, and α-quartz phases in the synthesis products. Both zeolites UTL and MTW represent intermediates in this reaction system prepared with an optimum reaction time of about six days for UTL and around ten days for MTW, respectively. However, under the reaction conditions used it was not possible to prepare phase-pure MTW zeolite. This was mainly due to the fact that the first diffraction lines of quartz were found in the X-ray patterns almost immediately after the appearance of diffraction lines of MTW zeolite.

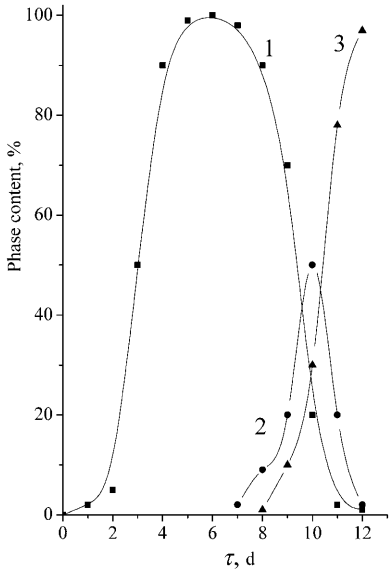

Figure 3. The effect of crystallization time on the crystallinity of germanosilicate UTL with Si/Ge = 2 and (Si + Ge)/SDA = 4: 1) UTL, 2) MTW, 3) quartz.

Based on the results obtained it can be concluded that the increase in the initial Si/Ge ratio from 2 to 5 does not lead to any significant change in the crystallinity of the UTL zeolite. Unfortunately, our attempts to synthesize the UTL zeolite from reaction mixtures with a Si/Ge ratio up to 10 were not successful: mostly zeolites with the STF structure were prepared. This is probably caused by the key role of germanium in the formation of D4R units, which are a very important part of the UTL structure, although they are not characteristic for aluminosilicate high-silica zeolites. Thus, the highest Si/Ge molar ratio in the product in UTL zeolites prepared under our reaction conditions was 9.44 (UTL/5). On the other hand, the excess of Ge in the reaction mixture causes the crystallization of a separate dense phase. It is necessary to consider also that reaction mixtures with high contents of germanium are more reactive than high-silica mixtures at the same pH value, and germanate zeolites are less stable. As a consequence, a faster UTL zeolite crystallization proceeds, followed by zeolite transformation into a dense phase for a longer synthesis duration.

An increase in the SDA concentration in the reaction mixture did not result in a change of the zeolite crystallinity, as shown by X-ray powder diffraction and the change of the structural type of the zeolite synthesized. The SDA was provided in the hydroxide form, thus, an increase in the SDA concentration was accompanied by an increase in the amount of hydroxide in the reaction mixture. Table 2 provides the micropore volumes of individual UTL samples synthesized with different Si/Ge and (Si + Ge)/SDA ratios for four and six days. The highest micropore volumes of 0.220 and 0.213 $cm^3 g^{-1}$ were determined for zeolites UTL/2 and UTL/7, respectively, prepared with (Si + Ge)/SDA equal to 1.7 and 2.4. Although the X-ray powder patterns of UTL/1 and UTL/2 after a six-day synthesis are of high quality,

Table 2. Structure parameters of calcined samples (RM = reaction mixture).

	Si/Ge in RM	(Si+Ge)/SDA in RM	S_{BET} [$m^2 g^{-1}$]	V_{total} [$cm^3 g^{-1}$]	V_{micro} [$cm^3 g^{-1}$]
UTL/1[a]	2	4	215	0.135	0.114
UTL/1	2	4	281	0.206	0.136
UTL/2[a]	2	1.7	326	0.163	0.152
UTL/2	2	1.7	417	0.234	0.220
UTL/5	5	4	347	0.236	0.155
UTL/6	1	4	52	0.111	0.022
UTL/7	2	2.4	469	0.220	0.213

[a] Samples with a four day synthesis.

there is a significant difference in the micropore volume: 0.136 versus 0.220 $cm^3 g^{-1}$. This indicates faster progress of the synthesis of UTL samples prepared with a higher amount of SDA, and therefore a higher concentration of hydroxide in the reaction mixture. The prolongation of the synthesis time for UTL/1 to 15 days was not sufficient to reach a micropore volume higher than 0.180 $cm^3 g^{-1}$. This again stresses the role of the hydroxide concentration in the reaction mixture. Preliminary results obtained with a mixture of hydroxide and bromide forms of the SDA confirm the importance of the concentration of hydroxide ions for the synthesis.

The results of X-ray powder diffraction and the chemical analysis of the UTL zeolite dried at temperature 90 °C show that in the range Si/Ge = 2–5 (in the reaction mixture), zeolites with the template contents 12.56–12.73 % are formed. In contrast, for sample UTL/6 with the increased germanium content, we observed a low amount of the SDA (Table 1) due to the presence of the additional β-GeO_2 phase and the blocking of channels by extra-framework germanium-containing species.

SEM images of UTL zeolites prepared under different chemical compositions of the reaction mixture (Figure 4) showed that the optimum Si/Ge ratio for the formation of a pure crystal phase with the UTL structure is Si/Ge = 2. After 4–6 days of the hydrothermal synthesis at 175 °C, homogeneous, rectangular (close to square), lamellar crystals of thickness 0.5–1 μm and average size about 10 × 10 μm were formed. The majority of crystals are isolated ones, and the minority consist of aggregates of lamellar crystals (Figure 4, top right). It should be noted that SEM, together with X-ray powder diffraction, confirms a high degree of crystallinity and phase purity of the prepared samples of UTL zeolites. The increase in the concentration of the SDA in a reaction mixture by 2.3 times did not cause any significant changes in the crystal morphology except for an increase in the average size of crystals up to 15 μm. The resulting morphology of the crystals under study differs from the morphology of IM-12 crystals described by Paillaud et al.[21] The authors reported on the formation of two types of crystals: large aggregates of size 150 × 150 × 150 μm under static synthesis conditions, and flower-type aggregates of thin crystals under agitation. In addition, the increase in the Si/Ge ratio up to 5 in the reaction mixture led to a substantial growth of the average size of crystals up to 20 × 40 × 5 μm (Figure 4, bottom right).

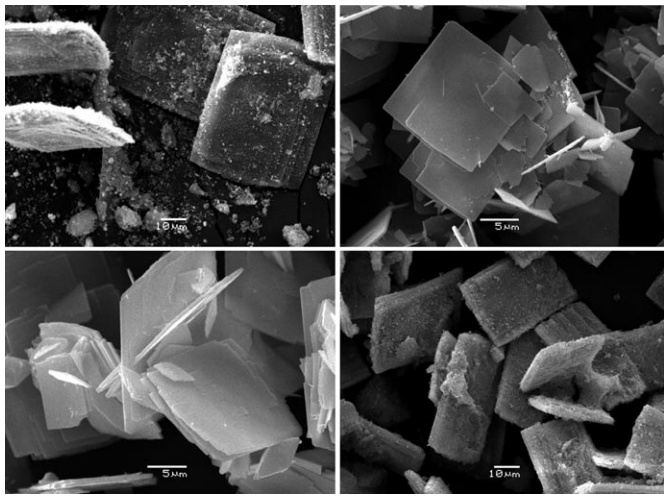

Figure 4. SEM images of calcined UTL samples obtained from reaction mixtures with different Si/Ge and (Si + Ge)/SDA ratios: top left: 1 and 4 (scale bar = 10 μm); top right: 2 and 4 (scale bar = 5 μm); bottom left: 2 and 1.7 (scale bar = 5 μm); bottom right: 5 and 4 (scale bar = 10 μm).

The reduction of the Si/Ge ratio in the reaction mixture to 1 led to a sharp increase in the average size of the UTL crystals up to 40 × 50 × 10 μm (Figure 4, top left). Some intergrowth of zeolite crystals with visible edge dislocation was observed. In this picture evidence of significant amounts of a secondary phase without a defined morphology is clearly provided. Based on the XRD data, the secondary phase in these samples was identified as β-GeO_2. The above given observations, together with the results obtained by other methods, allow us to draw the following conclusions concerning the crystallization of reaction mixtures with different Si/Ge ratios. With respect to the solubility of the reaction mixture, the rate of the gel recrystallization to germanium and silicon dioxide, and also the formation of competing phases under the conditions of hydrothermal treatment in the presence of (6*R*,10*S*)-6,10-dimethyl-5-azoniaspiro-[4.5]decane hydroxide, the optimum Si/Ge ratio in the reaction mixture should be in the range 1.5–3. For such a composition of the reaction mixture, a significant number of nuclei are formed, favoring the uniformity of crystal sizes and shapes and allowing the fast crystallization and full transformation of the gel into the zeolitic crystal phase.

FTIR spectra of the skeletal vibration region for zeolite with the UTL structure, synthesized with different template contents in the reaction mixture, are very similar; this allows a conclusion to be drawn on the insignificant influence of the template concentration in the range (Si + Ge)/SDA = 1.8–4 (Figure 5). The assignment of the infrared bands was based mainly on references [31,32]. The spectra show the presence of intensive stretching absorption bands at 1171 and 1241 cm^{-1} and bending vibrations at 525, 539, 578, and 594 cm^{-1} (Figure 5b). No significant redistribution of the intensities of pair bands at 525 and 539 m and 578 and

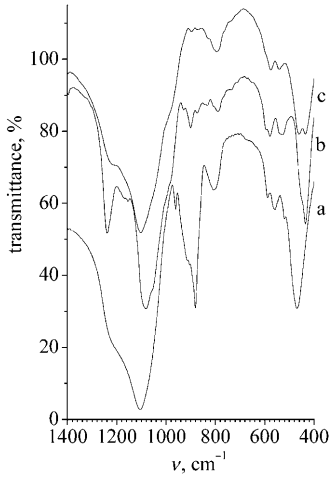

Figure 5. FTIR of skeletal vibrations of as-synthesized samples with UTL topology, Si/Ge = 1 (a), 2 (b), and 5 (c).

Figure 6. In general, for all samples the weight loss takes place in two steps. The first step is observed in the temperature range from ambient temperature up to 300–320 °C (depending on the Si/Ge ratio). This weight loss is due to the desorption of water from the zeolite. The second step, in the range 300–700 °C, corresponds to the SDA removal. Further weight loss above 700 °C is evidently caused by a partial dehydroxylation of UTL zeolites. Zeolites with the UTL structure showed very high thermal stability: their structure did not collapse even after calcinations at 1000 °C. Note that the temperature range of the dehydration depends on the Si/Ge ratio and can be explained by different surface hydrophobicity of the zeolite. In contrast, the temperature corresponding to the maximum of template removal is similar for all the UTL zeolites under study. A very low template content and relatively high amount of water were observed for UTL/6 with Si/Ge = 1. The probable reason is that, due to a high

594 cm^{-1} was observed for zeolites different in their Si/Ge ratio. This indicates that no additional deformations of the zeolite structure occurred as a change of the distribution of silicon and germanium in the framework proceeded. A shoulder in the spectrum found at 980 cm^{-1} could be assigned to the vibrations including Si–O–Ge moieties, and four absorption peaks at 930–835 cm^{-1} are associated with different type Ge–O–Ge species.

With increasing silicon content in UTL zeolites (Figure 5c) all structurally insensitive bands are shifted to a higher frequency area (it is particularly noticeable for the most intensive band of stretching vibrations shifting from 1082 up to 1105 cm^{-1}). The second observable feature relates to a significant decrease in the intensity of the structurally sensitive band at 1239 cm^{-1}, the intensity of the Ge–O stretching vibrations band at 930–835 cm^{-1}, and the appearance of a new Si–O–Si band at 460 cm^{-1}. The specified changes in the FTIR spectrum reflect, first of all, the essential increase in the silicon population in D4R positions. Significant reduction of the silicon contents in UTL samples also led to a significant increase in the intensity of the absorption bands at 960, 911, and 880 cm^{-1}, probably describing stretching vibrations of tetra- and penta-coordinated germanium with the oxygen environment.

The results of thermogravimetric analysis (TG, DTG) and differential thermal analysis (DTA) of zeolites with the UTL structure synthesized from various reaction mixtures are rather similar. TG, DTG, and DTA curves for zeolites with different Si/Ge and (Si+Ge)/SDA ratios are shown in

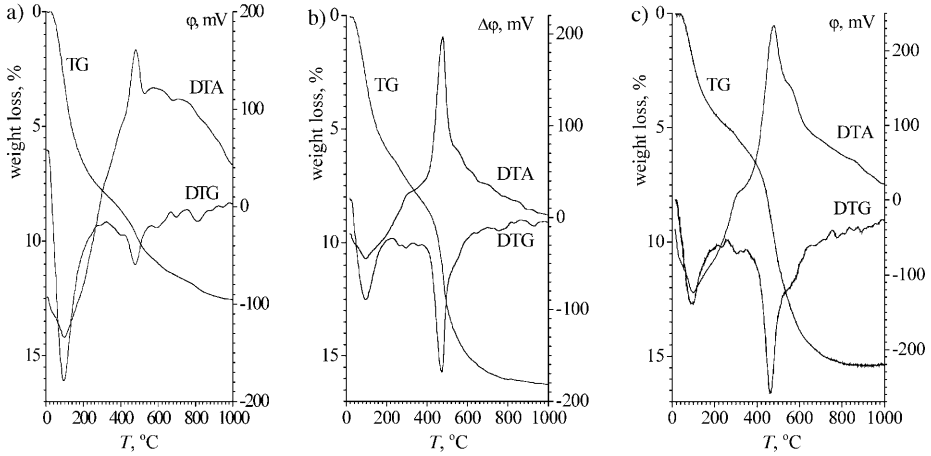

Figure 6. Thermogravimetric analysis of as-synthesized UTL samples. Si/Ge and (Si+Ge)/SDA ratio: a) 1 and 4, b) 2 and 4, c) 5 and 4, respectively.

concentration of Ge in the reaction mixture, GeO_2 has been partly formed together with the UTL zeolite.

Textural parameters of the porous structure of the UTL zeolites were determined by using adsorption isotherms, with nitrogen and argon as adsorbates (Figure 7). Sample UTL/6 (Si/Ge = 1) exhibited a low micropore volume (Table 2) due to the presence of a substantial amount of GeO_2, which is in good agreement with the X-ray diffraction pattern (cf. Figure 1, left). The micropore volume of studied zeolites with different Si/Ge ratio agrees well with the amount of template in as-synthesized samples (and CHN analysis data), but not with total weight loss data obtained from the thermal analysis investigation.

The analysis of N_2 and Ar adsorption isotherms in a pressure range from 10^{-6} to 4.10^{-1} p/p_s allowed us to determine micropore size distributions for the calcined samples. Calculation from adsorption isotherms of nitrogen carried out by using the DFT approach[33] and the Saito–Foley[34] method showed the average pore diameter to be close to 1.05 and

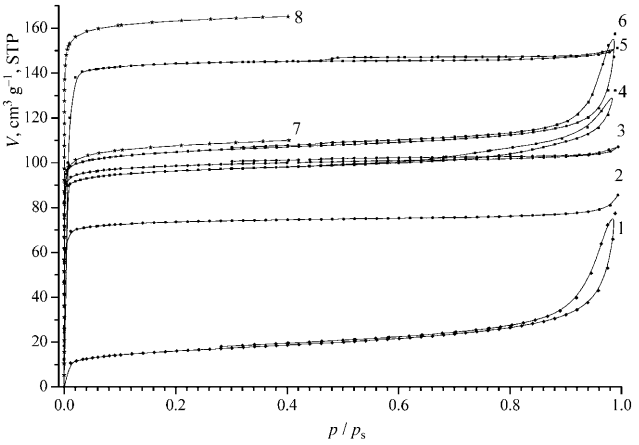

Figure 7. Adsorption isotherms of nitrogen (1–6) and argon (7 and 8) for samples of UTL zeolite (see Table 1 and Table 2): 1) UTL/6, 2) UTL/1, 3) UTL/2 (4-day synthesis), 4,7) UTL/1, 5,8) UTL/2, 6) UTL/5.

1.10 nm, respectively (Figure 8). Analysis of the Ar adsorption isotherm by using the Saito–Foley (SF) method showed

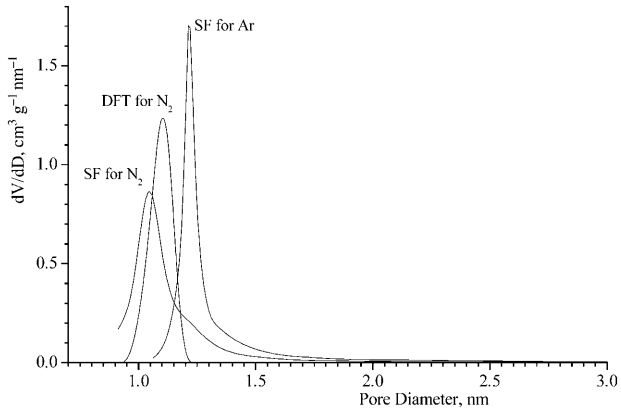

Figure 8. Pore size determination for best porosity sample (UTL/2).

the diameter was close to 1.20 nm. It is known that the pore diameter value is very sensitive with regard to the values of magnetic susceptibility and polarizability.[33] Argon is usually preferred due to its spherical shape, but the value obtained from argon measurements is higher than that from X-ray powder diffraction. It is important to note that only one maximum has been obtained, even without any shoulder. This indicates that even a high-resolution argon measurement is not able to distinguish between two types of pores with diameters of 8.5×5.5 and 9.5×7.1 Å, and the obtained pore size was a little overestimated. Considering this, it appears that the results of nitrogen and argon adsorption are in good agreement with the data of the X-ray structure analysis, and confirm that the investigated zeolites possess extra-large pores.

Conclusion

A number of silicogermanate zeolites with UTL topology have been synthesized in alkaline media using (6*R*,10*S*)-6,10-dimethyl-5-azoniaspiro[4.5]decane hydroxide as the structure-directing agent. The optimum synthesis time was found to be six days for Si/Ge and (Si+Ge)/SDA molar ratios of 2 and 1.7, respectively. The typical Si/Ge ratio in solid samples is 4.17, but it can be increased up to 9–10 without an essential decrease of zeolite crystallinity. Zeolite with the UTL structure shows very high thermal stability: the structure did not collapse after calcinations at 1000 °C. The micropore volume of the best crystals is 0.22 $cm^3 g^{-1}$, and the micropore diameter is 1.05 nm.

Experimental Section

Synthesis of the structure-directing agent: Preparation of the (6*R*,10*S*)-6,10-dimethyl-5-azoniaspiro[4.5] decane hydroxide (Scheme 1) was performed according to the following procedure. Distilled water (140 mL), sodium hydroxide (5.68 g, Lach-Ner, Czech Republic), and 1,4-dibromobutane (30.66 g, Aldrich) were mixed in a round-bottom flask. Then, (2*R*,6*S*)-2,6-dimethylpiperidine (16.07 g, Aldrich) was added dropwise

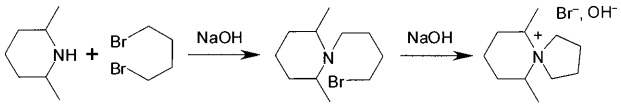

Scheme 1. Template preparation.

over a period of 30 min under reflux. The mixture was vigorously stirred (≈1000 rpm) for 12 h to prepare a milklike suspension. Then, the mixture was cooled down in an ice bath. The temperature was decreased, and an ice-cooled solution of sodium hydroxide (70 mL, 50 wt%) was added. After that, solid sodium hydroxide (20 g) was added slowly under vigorous stirring and further cooling by ice. The addition of sodium hydroxide was stopped after an appearance of the oil product. Further intensive stirring led to the formation of the crystalline phase, which was recovered by filtration and extracted three times with chloroform (100 mL). The organic fractions were dried using anhydrous sodium sulfate and partially evaporated. The ammonium salt was precipitated and washed out with diethyl ether. The salt was converted into hydroxide form by ion exchange with AG 1-X8 resin (Bio-Rad). The yield of the product was about 92%. The successful synthesis of the structure-directing agent was confirmed by NMR spectroscopy after dissolution in [D_6]dimethyl sulfoxide.

Synthesis of germanosilicate with UTL structure: The synthesis of zeolite with UTL topology was carried out by a modified method described in reference [20]. Reaction gel of molar composition: 0.6–1.0 SiO_2/0.6–0.2 GeO_2/0.3–0.7 SDA/30–33 H_2O was prepared by dissolving amorphous germanium oxide (Aldrich) in the solution of SDA. A list of individual samples with their abbreviations and specified molar ratios of individual reaction components is provided in Table 1. After that, silica (Cab-O-Sil M5) was added into the solution and the mixture was stirred at room temperature for 30 min. The resulting fluid gel was charged into 25 mL Teflon-lined home-made stainless steel autoclaves and heated at 175 °C for 3–9 days under agitation (40 rpm). The solid product was recovered by filtration, thoroughly washed with distilled water and dried overnight at 90 °C.

To remove the SDA, the as-synthesized zeolite was calcined in air at 550 °C for 6 h with a temperature ramp of 1 °C min^{-1}.

Characterization: X-ray powder diffraction data were obtained on a Bruker AXS D8 diffractometer in the Bragg–Brentano geometry by using $Cu_{K\alpha}$ radiation with a graphite monochromator and a position-sensitive detector (Vantec-1). The relative crystallinity of individual zeolite samples was determined using the diffraction line at 6.23° with (*hkl*) index (200). To limit the effect of preferential orientation of individual UTL crystals, being aware of their shapes (see Figure 4), a gentle grinding of the samples was carried out to decrease their size, and they were packed carefully into the holder.

The content of Si and Ge was determined on a Philips PW 1404 X-ray fluorescence spectrometer. Calcined samples were homogenized using agate mortar, and after adding dentacryle as a binder they were deposited on a surface of cellulose tablets.

The morphology of zeolite particles was evaluated using a scanning electron microscope JEOL JSM-5500 LV.

FTIR spectra of skeletal vibrations of ITQ-15 samples were recorded on an FTIR spectrometer Nicolet Protégé 460 by using a KBr pellet technique.

Thermogravimetric analysis (TGA) and differential thermal analysis (DTA) were performed on a Q-1000 thermal analyzer (MOM, Hungary) from room temperature to 1000 °C with a heating rate of 10 °C min^{-1} under flowing air.

Adsorption isotherms of argon and nitrogen at −196 °C were measured with a Micromeritics ASAP 2020 instrument. Prior to the adsorption measurements, all samples were degassed at 250 °C until a pressure of 0.001 Pa was attained. Nitrogen and argon were used as adsorbates to properly evaluate the pore size of this microporous germanosilicate. The micropore size distribution was calculated by using DFT[33] and Saito–Foley[34] methods for cylinder pore geometry.

^{1}H NMR (300 MHz) spectra used for characterization of the structure-directing agent prepared were recorded on a Varian Mercury 300 spectrometer in [D_6]dimethyl sulfoxide at 25 °C (data are not shown here).

Acknowledgement

A.Z. thanks the Academy of Sciences of the Czech Republic (1QS400400560) and J.Č. thanks the Grant Agency of the Czech Republic (203/08/0604) for the financial support of this work.

[1] J. Čejka, B. Wichterlová, *Catal. Rev.* **2002**, *44*, 375–421.
[2] T. Maesen, *Stud. Surf. Sci. Catal.* **2007**, *168*, 1–12.
[3] K. Tanabe, W. F. Hölderich, *Appl. Catal. A* **1999**, *181*, 399–434.
[4] S. I. Zones, C. Y. Chen, A. Corma, M. T. Cheng, C. L. Kibby, I. Y. Chan, A. W. Burton, *J. Catal.* **2007**, *250*, 41–54.
[5] B. Wichterlová, J. Čejka, *Catal. Lett.* **1992**, *16*, 421–429.
[6] J. Čejka, N. Žilková, B. Wichterlová, G. Eder-Mirth, J. A. Lercher, *Zeolites* **1996**, *17*, 265–271.
[7] C. W. Jones, S. I. Zones, M. E. Davis, *Microporous Mesoporous Mater.* **1999**, *28*, 471–481.
[8] S. Zheng, A. Jentys, J. A. Lercher, *J. Catal.* **2006**, *241*, 304–311.
[9] S. Al-Khattaf, N. M. Tukur, A. Al-Amer, U. A. Al-Mubaiyedh, *Appl. Catal. A* **2006**, *305*, 21–31.
[10] L. Červený, K. Mikulcová, J. Čejka, *Appl. Catal. A* **2002**, *223*, 65–72.
[11] P. Botella, A. Corma, M. T. Navarro, F. Rey, G. Sastre, *J. Catal.* **2003**, *217*, 406–416.
[12] J. Čejka, *Stud. Surf. Sci. Catal.* **2005**, *157*, 111–134.
[13] P. Wagner, M. Yoshikawa, M. Lovallo, K. Tsuji, M. Taspatsis, M. E. Davis, *Chem. Commun.* **1997**, 2179–2180.
[14] R. F. Lobo, M. Tsapatsis, C. C. Freyhardt, S. Khodabandeh, P. Wagner, C. Y. Chen, K. J. Balkus, S. I. Zones, M. E. Davis, *J. Am. Chem. Soc.* **1997**, *119*, 8474–8484.
[15] A. Burton, S. Elomari, C. Y. Chen, R. C. Medrud, I. Y. Chan, L. M. Bull, C. Kibby, T. V. Harris, S. I. Zones, E. S. Vittoratos, *Chem. Eur. J.* **2003**, *9*, 5737–5748.
[16] K. G. Strohmaier, D. E. W. Vaughan, *J. Am. Chem. Soc.* **2003**, *125*, 16035–16039.
[17] A. Corma, M. J. Díaz-Cabañas, J. L. Jorda, C. Martines, M. Moliner, *Nature* **2006**, *443*, 842–845.
[18] C. H. Christensen, K. Johannsen, I. Schmidt, C. H. Christensen, *J. Am. Chem. Soc.* **2003**, *125*, 13370–13371.
[19] J. Čejka, S. Mintova, *Catal. Rev. Sci. Eng.* **2007**, *49*, 457–509.
[20] A. Corma, M. J. Díaz-Cabañas, F. Rey, S. Nicolopoulus, Kh. Boulahya, *Chem. Commun.* **2004**, 1356–1357.
[21] J.-L. Paillaud, B. Harbuzaru, J. Patarin, N. Bats. *Science* **2004**, *304*, 990–992.
[22] A. Corma, M. T. Navarro, F. Rey, J. Rius, S. Valencia, *Angew. Chem.* **2001**, *113*, 2337–2340; *Angew. Chem. Int. Ed.* **2001**, *40*, 2277–2280.
[23] A. Corma, M. T. Navarro, F. Rey, S. Valencia, *Chem. Commun.* **2001**, 1720–1721.
[24] A. Corma, F. Rey, S. Valencia, J. L. Jorda, J. Rius, *Nat. Mater.* **2003**, *2*, 493–497.
[25] D. L. Dorset, G. J. Kennedy, K. G. Strohmaier, M. J. Diaz-Cabanas, F. Rey, A. Corma, *J. Am. Chem. Soc.* **2006**, *128*, 8862–8867.
[26] G. Sastre, A. Pulido, A. Corma, *Microporous Mesoporous Mater.* **2005**, *82*, 159–163.
[27] US patent 6797254 (2004).
[28] A. Corma, M. J. Diaz-Cabanas, J. Martínez-Triquero, F. Rey, J. Rius, *Nature* **2002**, *418*, 514–517.
[29] A. Corma, M. J. Diaz-Cabanas, F. Rey, *Chem. Commun.* **2003**, 1050–1051.
[30] R. Castaneda, A. Corma, V. Fornes, F. Rey, J. Rius, *J. Am. Chem. Soc.* **2003**, *125*, 7820–7821.
[31] T. Conradsson, X. Zou, M. S. Dadachov, *Inorg. Chem.* **2000**, *39*, 1716–1720.
[32] Y. Li, X. Zou, *Angew. Chem.* **2005**, *117*, 2048–2051; *Angew. Chem. Int. Ed.* **2005**, *44*, 2012–2015.
[33] S. Lowell, J. E. Shields, M. A. Thomas, M. Thommes, *Characterization of Porous Solids and Powders: Surface Area, Pore Size and Density*, Kluwer, Dordrecht **2004**, p. 145, 148.
[34] A. Saito, H. C. Foley, *AIChE J.* **1991**, *37*, 429–436.

Received: March 7, 2008
Revised: June 23, 2008
Published online: September 11, 2008

